https://doi.org/10.5607/en22005
Exp Neurobiol. 2022 Oct;31(5):307-323.
pISSN 1226-2560 • eISSN 2093-8144

Original Article

Experimental Neurobiology

Lipopolysaccharide-induced Autophagy Increases SOX2-positive Astrocytes While Decreasing Neuronal Differentiation in the Adult Hippocampus

Wen-Chung Liu[1,2†], Chih-Wei Wu[1,3†], Mu-Hui Fu[4], You-Lin Tain[5,6,7], Chih-Kuang Liang[8], I-Chun Chen[5], Chun-Ying Hung[5], Yu-Chi Lee[5] and Kay L.H. Wu[5,9*]

[1]Department of Plastic Surgery, Kaohsiung Veterans General Hospital, Kaohsiung 813414, [2]Department of Surgery, School of Medicine, National Yang Ming Chiao Tung University, Taipei 112034, [3]Department of Counseling, National Chia-Yi University, Chia-Yi 621, [4]Department of Neurology, Kaohsiung Chang Gung Memorial Hospital, Chang Gung University College of Medicine, Kaohsiung 83301, [5]Institute for Translational Research in Biomedicine, Kaohsiung Chang Gung Memorial Hospital, Kaohsiung 83301, [6]Department of Pediatrics, Kaohsiung Chang Gung Memorial Hospital, Chang Gung University College of Medicine, Kaohsiung 83301, [7]College of Medicine, Chang Gung University, Taoyuan 330, [8]Center for Geriatrics and Gerontology, Division of Neurology, Kaohsiung Veterans General Hospital, Kaohsiung 813414, [9]Department of Senior Citizen Services, National Tainan Institute of Nursing, Tainan 700, Republic of China

Inflammation alters the neural stem cell (NSC) lineage from neuronal to astrogliogenesis. However, the underlying mechanism is elusive. Autophagy contributes to the decline in adult hippocampal neurogenesis under *E. coli* lipopolysaccharide (LPS) stimulation. SRY-box transcription Factor 2 (SOX2) is critical for NSC self-renewal and proliferation. In this study, we investigated the role of SOX2 in induced autophagy and hippocampal adult neurogenesis under LPS stimulation. LPS (5 ng•100 g^{-1}•$hour^{-1}$ for 7 days) was intraperitoneally infused into male Sprague–Dawley rats (8 weeks old) to induce mild systemic inflammation. Beclin 1 and autophagy protein 12 (Atg12) were significantly upregulated concurrent with decreased numbers of Ki67- and doublecortin (DCX)-positive cells in the dentate gyrus. Synchronically, the levels of phospho(p)-mTOR, the p-mTOR/mTOR ratio, p-P85s6k, and the p-P85s6k/P85s6k ratio were suppressed. In contrast, SOX2 expression was increased. The fluorescence micrographs indicated that the colocalization of Beclin 1 and SOX2 was increased in the subgranular zone (SGZ) of the dentate gyrus. Moreover, increased S100β-positive astrocytes were colocalized with SOX2 in the SGZ. Intracerebroventricular infusion of 3-methyladenine (an autophagy inhibitor) effectively prevented the increases in Beclin 1, Atg12, and SOX2. The $SOX2^+$-$Beclin\ 1^+$ and $SOX2^+$-$S100\beta^+$ cells were reduced. The levels of p-mTOR and p-P85s6k were enhanced. Most importantly, the number of DCX-positive cells was preserved. Altogether, these data suggest that LPS induced autophagy to inactivate the mTOR/P85s6k pathway, resulting in a decline in neural differentiation. SOX2 was upregulated to facilitate the NSC lineage, while the autophagy milieu could switch the SOX2-induced NSC lineage from neurogenesis to astrogliogenesis.

Key words: Autophagy, SOX2, mTOR signaling, Adult hippocampal neurogenesis, Lipopolysaccharide

INTRODUCTION

As final differentiated cells, mature neurons lose the ability to generate new neurons, contributing to the lack of a cure for neurodegeneration. Fortunately, a group of neural stem cells (NSCs) are preserved in the dentate gyrus of the hippocampus to generate new neurons in the adult mammal [1, 2]. The process of the trans-

Submitted January 27, 2022, Revised September 28, 2022, Accepted October 9, 2022

*To whom correspondence should be addressed.
TEL: 886-7-7317123 (ext. 8596), FAX: 886-7-7317123 (ext. 8569)
e-mail: klhwu@cgmh.org.tw
†These authors contributed equally to this article.

formation from neuronal stem cells (NSCs) to neural progenitor cells (NPCs) required for neural differentiation and maturation in adulthood is known as adult neurogenesis [3]. These newborn neurons integrate into the existing circuit of the hippocampus to maintain and improve learning and memory function [4-11]. Along the birth of new neurons, NSCs also produce astrocytes [12, 13]. Inflammation alters NSC differentiation and leads to a shift in linage from neuronal to astrogliogenesis [14, 15], resulting in decreased newborn neurons. However, the underlying mechanisms are inconclusive.

Systemic administration of lipopolysaccharide (LPS) induces autophagy [16] and impairs NSC proliferation and differentiation in the adult hippocampus [2, 17-19]. Autophagy, which progresses the degradation of unwanted cell components, is initiated by the nucleation and elongation of phagophores. The formation of the autophagosomal membrane is mediated by the Class III PI3K complex, Beclin 1 with a multiprotein complex, while autophagy protein 12 (Atg12) conjugates to Atg5 for the formation of phagophores for further protein engulfment or organelle degradation [20]. Although autophagy-mediated astrogliogenesis in adult hippocampal neural stem cells has been documented [21], the underlying mechanism is still inconclusive.

In contrast to autophagy, accumulating evidence suggests that mTOR/s6k signaling governs protein synthesis to activate cell growth and division [22, 23]. After activation, mTOR activates s6k by phosphorylation to support neuronal differentiation [24, 25]. To date, the following two major isoforms of s6k have been identified: P70s6k, which is the cytoplasmic isoform, and P85s6k, which is the nuclear isoform [26]. Whether the wax and wane of autophagy and mTOR signaling occur in the hippocampus under LPS is unclear.

SOX2 is a transcription factor crucial for promoting the self-renewal and proliferation of NSCs [27]. Recently, SOX2-positive cells colocalized with autophagosomes were detected in the dentate gyrus of animals under stress [28]. Notably, SOX2 is widely expressed in hippocampal astrocytes [12]. These lines of evidence indicate the possibility that SOX2 might mediate LPS-induced autophagy to reduce neuron differentiation by inducing astrocyte production. Nonetheless, the interplay among SOX2 in LPS-induced autophagy, mTOR/s6k signaling, and adult hippocampal neurogenesis is unclear.

Peripheral or central LPS administration is a well-accepted model used to investigate the stress-associated decline in adult neurogenesis. Sustained, lower grade LPS administration is related to a mild level of systemic inflammation, such as microbiota dysbiosis [29, 30]. In this study, we examined the contribution of SOX2 and autophagy to the decline in adult neurogenesis in the hippocampus by using a rodent model of sustained, low-level *E. coli* lipopolysaccharide (LPS) peritoneal infusion (IP) mimicking microbiota dysbiosis-associated LPS increments [29, 30]. 3-Methyladenine (3MA, a common inhibitor of autophagy) or vehicle was intracerebroventricularly (icv) infused for seven days. The protein expression and distribution of the autophagy factors mTOR signaling, SOX2, cell proliferation, and neuronal differentiation in the dentate gyrus of the hippocampus were detected to identify the roles of autophagy and SOX2 in LPS-decreased adult neurogenesis.

MATERIALS AND METHODS

Male, 7-week-old Sprague–Dawley rats (SD from the Experimental Animal Center, National Science Council, Taiwan) were used in this study and allowed to acclimatize in a temperature- (22±1℃) and light- (12:12 light-dark cycle, light on from 08:00) controlled animal room for one week before the experiments. All experiments were carried out in accordance with the guidelines for animal experimentation endorsed by the Institutional Animal Care and Use Committee (IACUC) of Kaohsiung Chang Gung Memorial Hospital. The animals consumed regular chow *ad libitum* as the only food source. Their body weight and food and liquid intake per cage were measured and recorded each week. *Escherichia coli* LPS was intraperitoneally infused, and 3-methyladenine (3MA) was intracerebroventricularly infused (icv) by an osmotic minipump for 7 days. After deep anesthetization and transcardial perfusion with sterile saline, the forebrain was sampled for further study. A schematic depicting the study design is shown in Fig. 1.

Implantation of osmotic minipump of lipopolysaccharide

Regarding the intraperitoneal infusion (IP), systemic inflammation was induced by continuous intraperitoneal infusion via an osmotic minipump of LPS (5 ng•100 g^{-1}•$hour^{-1}$ for 7 days; Sigma–Aldrich, St. Louis, MO, USA). On the day of implantation, animals were anesthetized with sodium pentobarbital (50 mg/kg, IP), and

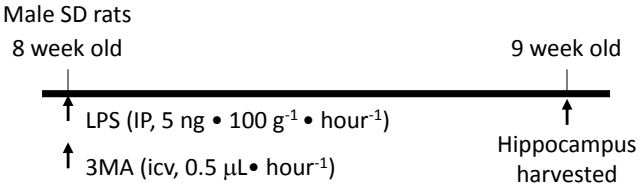

Fig. 1. Schematic illustration of the study design used to establish a sustained, low-grade systemic infection rodent model by peritoneal infusion (IP) of LPS (5 ng•100 g^{-1}•$hour^{-1}$ for 7 days) in 8-week-old male Sprague–Dawley rats treated with vehicle or 3MA intracerebroventricular infusion (icv) for 7 days. 3MA: 3-Methyladenine.

https://doi.org/10.5607/en22005

osmotic minipumps (ALZET® Micro-Osmotic Pump Model 1007D; Durect, Cupertino, CA, USA) were placed in the peritoneal cavity. Control animals received saline-filled osmotic minipumps, and the sham-operated animals underwent identical surgical procedures with the implantation of a vehicle-filled osmotic minipump. Following implantation, the abdominal muscles were closed in layers, and body temperature was maintained at 37℃ with a heating pad until the animals recovered from anesthesia.

Intracerebroventricular infusion

Regarding the animals that received additional central infusion of the test agents, rats were placed in a sealed Plexiglas box into which 4% isoflurane and 2 L/min oxygen flow were introduced for anesthesia. Then, the rats were placed in a standard stereotaxic device equipped with a gas anesthesia nose cover to maintain anesthesia throughout the surgery with 2% isoflurane and 600 ml/min oxygen flow. A drug-filled osmotic pump was surgically implanted with an ALZET Brain Infusion probe (Alzet 1002) into the right lateral ventricle with the tip of the infusion probe at the following coordinates with reference to Bregma: anterior/posterior -1.4 mm; medial/lateral 1.8 mm; and dorsal/ventral -3.0 mm (Paxinos and Watson, 2013 [31]). Intracerebroventricular infusion (icv) of 3MA (5 mM, infusion rate: 0.5 μl/hour, ALZET® MICRO-OSMOTIC PUMP MODEL 1007D) was carried out for 7 days. An infusion of sterile saline (Sal) served as the volume and vehicle control. Only animals that showed progressive weight gain after the operation were used in the subsequent experiments.

Immunofluorescence

To identify the distribution of SOX2 and Beclin 1, the forebrains were sampled and postfixed in 4% paraformaldehyde for 72 hours at 4℃ after transcardial perfusion. Furthermore, the forebrains were cryoprotected with 30% sucrose solution. Then, the forebrains were sliced with a freezing microtome at a thickness of 30 μm. The paraformaldehyde-fixed brain sections were stained with mouse anti-SOX2 (1:1,000, Abcam, CA), Beclin 1 (1:500, Cell Signaling), phospho(p)-mTOR (1:500, Sigma–Aldrich), or p-s6k (1:500, Cell Signaling), followed by goat anti-doublecortin (DCX, 1:750; Abcam, CA) for immature neurons, and rabbit anti-S100β (1:500, Novus Biologicals, CO) for astrocytes. 4',6-diamidino-2-phenylindole (DAPI) was employed to identify the morphology of the cell nuclei. The images were visualized, acquired, and processed under a confocal laser-scanning microscope (Olympus FLUOVIEW 10i-LIV, Tokyo, Japan) with a 60X oil immersion objective. The fluorescence intensity of SOX2, Beclin 1, p-mTOR, and p-s6k signals was detected in every 8th section for each rat and three rats for each group. The immunofluorescence intensity of each section was analyzed by ImageJ software (NIH, MD, USA). The process was modified from Mardhiyah et al., 2021 [24]. In brief, first - opening the image file, second - converting the RBG into the 8-bit channel, third – automatically adjusting the threshold, 4th - selecting the region of interest, 5th – calibrating and setting measurement from the analyze path, and 6th - intensity measurement. The intensity of the detected immunofluorescence was expressed as the area and raw intensity (RawIntDen). For co-localization, only the fluorescent signals located in the subgranular zone of the dentate gyrus were counted.

Immunohistochemistry for cell counts

For the cell counting analysis, the forebrains were sampled and postfixed in 4% paraformaldehyde for 72 hours at 4℃ after transcardial perfusion. Furthermore, the forebrains were cryoprotected with 30% sucrose solution. Then, the forebrains were sliced with a freezing microtome at a thickness of 30 μm. The paraformaldehyde-fixed brain sections were stained with mouse anti-Ki67 (1:1,000, Abcam, CA) for newly proliferated cells and goat anti-doublecortin (DCX, 1:750; Abcam, CA) for immature neurons. Immunohistochemical staining was performed using a Vectastain ABC system (Vector Laboratories, Burlingame, CA) and nickel-enhanced diaminobenzidine incubation. The images were acquired and processed under an Olympus light microscope (BX51, Tokyo, Japan).

Cell counting

The entire hippocampal dentate gyrus was sliced into an average of 193 coronal sections at a thickness of 30 μm. The numbers of Ki67- and DCX-positive cells, which were stained black, were counted in every 6th section. Only the Ki67-positive cells located in the subgranular zone of the dentate gyrus were counted as the targeted proliferation cells. The total number of labeled cells per section was determined and divided by the slide selection ratio to obtain the total number of labeled cells per dentate gyrus [19].

Total protein extraction

For the Western blot and ELISA analyses, the procedures were conducted as previously described [25, 26, 32]. In brief, the animals were deeply anesthetized with sodium pentobarbital (100 mg/kg; Sigma) and perfused with phosphate-buffered saline. The fresh brains were dissected, and tissue samples from the hippocampus were homogenized with a Dounce grinder and a tight pestle in ice-cold lysis buffer (15 mM HEPES, pH 7.2, 60 mM KCl, 10 mM NaCl, 15 mM $MgCl_2$, 250 mM sucrose, 1 mM EGTA, 5 mM EDTA, 1 mM PMSF, 2 mM NaF, and 4 mM Na_3VO_4). A mixture of leupeptin (8 μg/ml), aprotinin (10 μg/ml), phenylmethylsulfonyl

fluoride (20 μg/ml), and trypsin inhibitor (10 μg/ml) was included in the isolation buffer to prevent protein degradation. The homogenate was centrifuged at 13,500 *rpm* for 15 minutes, and the supernatant was collected for protein analysis. The concentration of the total protein extracted was estimated by the Bradford method with a protein assay kit (Bio-Rad, Hercules, CA).

Western blot analysis

The proteins of interest in the hippocampus were separated by using 10~12% SDS–PAGE. The samples from each group contained equivalent total protein concentrations. The proteins were electrophoretically transferred onto polyvinylidene difluoride (PVDF) membranes (Immobilon-P membrane; Millipore; Bedford, MA, USA). The membranes were probed with specific antibodies against Beclin-1 (1:1,000, Cell Signaling), Atg5 (1:1,000, Cell Signaling), Atg12 (1:1,000, Cell Signaling), SQSTM1 (1:1,000, Cell Signaling), LC3B (1:1,000, Sigma-Aldrich), mTOR (1:1,000, Cell Signaling), phospho(p)-mTOR (1:1,000, Sigma–Aldrich), P70s6k (1:1,000, Cell Signaling), p-P70s6k (1:1,000, Cell Signaling), P85s6k (1:1,000, Cell Signaling), and p-P85s6k (1:1,000, Cell Signaling). Then, the membranes were incubated with the appropriate horseradish peroxidase–conjugated secondary antibody. Specific antibody-antigen complexes were detected using an enhanced chemiluminescence Western blot detection system (Thermo Fisher Bioscience). The bands of the targeted proteins were densitometric quantified by ImageJ software (NIH, MD, USA), and the amounts of detected proteins are expressed as the ratio to β-actin protein.

Statistical analysis

All values are expressed as the mean±SEM. For the biochemical experiments involving multiple groups, one-way analysis of variance with repeated measures was used to assess the group means. This analysis was followed by a Tukey multiple range test as a *post hoc* assessment of the individual means. $p<0.05$ was considered statistically significant.

RESULTS

The LPS-induced increase in Beclin 1 and Atg12 in the hippocampus was reversed by 3MA intracerebroventricular infusion

LPS (5 ng•100 g^{-1}•$hour^{-1}$ for 7 days, IP) was administered to 8-week-old male Sprague Dawley rats to induce sustained, low-grade systemic infection concurrent with 3MA (a Class III PI3K inhibitor) icv infusion for 7 days (Fig. 1). The hippocampus was harvested at the end of the experiment for Western blot analyses. The results indicated that the expression levels of Beclin 1 (Fig. 2A; an essential factor for the nucleation of autophagy [33]) and Atg12 (Fig. 2C; an ubiquitin-like protein that contributes to autophagy vesicle formation [20, 34]) in the hippocampus were significantly upregulated by LPS administration. As a key factor for autophagosome formation, SQSTM1 directly binds LC3 to facilitate protein degradation by autophagy [35]. The results of the Western blot analyses further indicated that the expression levels of SQSTM1 (Fig. 2D), LC3B-I (Fig. 2E), and LC3B-II (Fig. 2F) were significantly enhanced in the LPS group. The 3MA treatment effectively abrogated these increases in Beclin 1 (Fig. 2A), Atg12 (Fig. 2C), SQSTM1 (Fig. 2D), and LC3B-II (Fig. 2F), while the increase in LC3B-I (Fig. 2E) was not reduced by 3MA. On the other hand, Atg5 did not significantly differ between groups (Fig. 2B). These results indicate that peritoneal LPS administration triggered the upregulation of hippocampal autophagy in seven days.

3MA prevented LPS-decreased cell proliferation and neuronal differentiation in the dentate gyrus

The cell counts of Ki67 (a marker of dividing cells)-positive cells and doublecortin (DCX, a marker of immature newborn neurons)-positive cells in the subgranular zone of the dentate gyrus were counted on Day 7 after LPS infusion. The results indicate that the numbers of dividing cells (Fig. 3A) and newborn neurons (Fig. 3B) were significantly reduced in the LPS group compared with those in the control group (Sal).

In the 3MA treatment group (L+3MA), the number of DCX-positive cells in the dentate gyrus was effectively maintained at the control level compared with that in the LPS group (Fig. 3B). On the other hand, 3MA had no significant effect on preventing the loss of Ki67-positive cells compared with the LPS group (Fig. 3A). These results suggest that LPS might decrease cell proliferation and differentiation in the hippocampus through different pathways. In particular, autophagy might mediate the decline in neuronal differentiation instead of cell proliferation.

3MA prevented LPS-downregulated mTOR signaling in the hippocampus

The mammalian target of rapamycin (mTOR), a central cell-growth regulator, inhibits autophagy [36]. To examine whether mTOR signaling was suppressed concurrent with LPS-enhanced autophagy, mTOR signaling was detected by Western blot analysis. The results indicated that the levels of total mTOR showed a decreasing trend in the LPS group, although no statistically significant difference was detected (Fig. 4A). On the other hand, expression of phospho(p)-mTOR (Fig. 4B) was significantly decreased

https://doi.org/10.5607/en22005

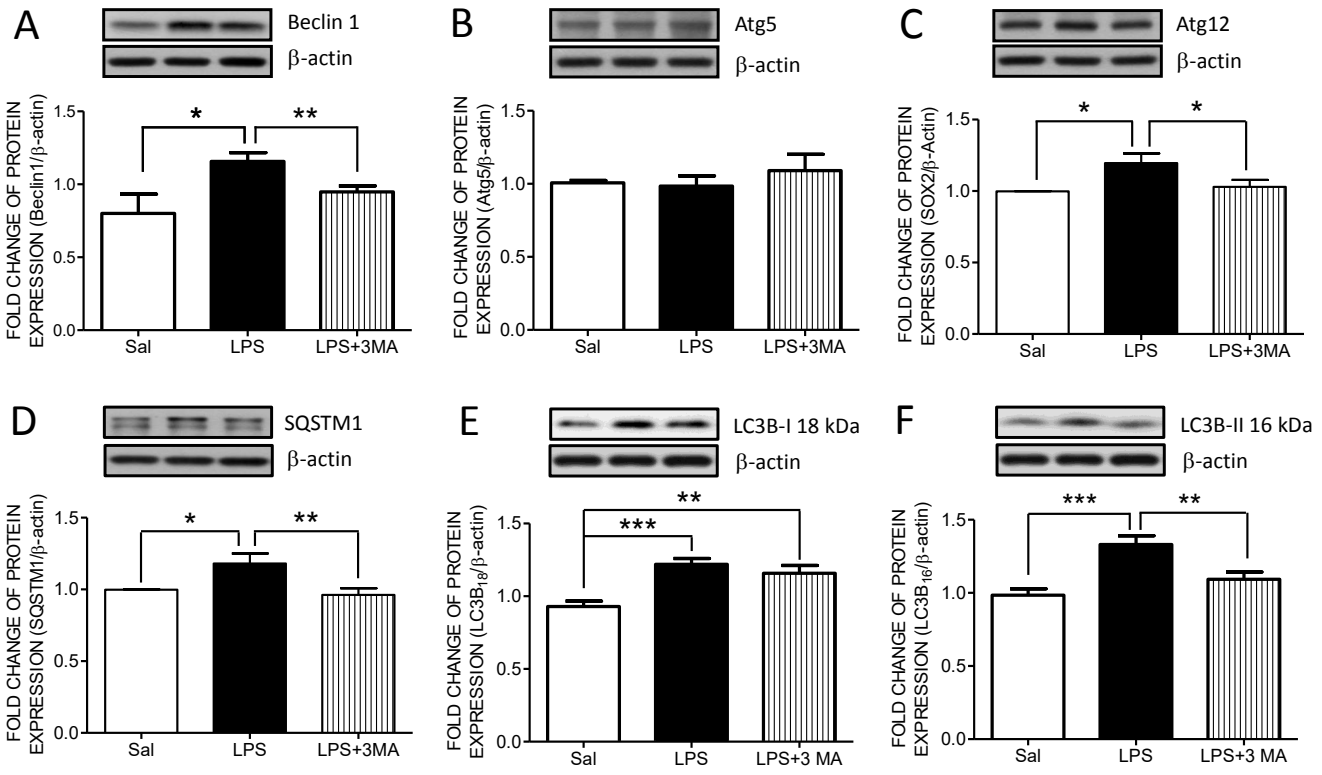

Fig. 2. The increased protein expression of autophagy signaling in the hippocampus induced by LPS administration was prevented by icv infusion of 3MA. Representative gels (inset) and densitometric analysis of the Western blot results showing changes in the expression of (A) Beclin 1, (B) Atg5, (C) Atg12, (D) SQSTM1, (E) LC3B-I, and (F) LC3B-II. Values are the mean±SEM, n=10 to 12 animals per experimental group. *p<0.05, **p<0.01, **p<0.001 in the *post hoc* Tukey's multiple range tests. Sal: vehicle infusion, LPS: LPS (IP) with vehicle (icv), LPS+3MA: LPS (IP) infusion with 3MA (icv).

in the LPS group. To further determine whether the decrease in p-mTOR was a result of mTOR reduction or inactivation of mTOR, the ratio of p-mTOR/mTOR was further evaluated. The results indicated that p-mTOR/mTOR was significantly reduced in the LPS group (Fig. 4C), suggesting inactivation of mTOR in the hippocampus under LPS administration. The reduced p-mTOR and p-mTOR/mTOR ratios imply a decrease in mTOR activation in the hippocampus by LPS stimulation. The 3MA icv infusion effectively prevented the reduced p-mTOR and p-mTOR/mTOR ratio.

Activated mTOR phosphorylates s6k, the downstream signal for protein synthesis, to support neuronal differentiation [24, 25]. There are two major isoforms of s6k as follows: P70s6k, which is the cytoplasmic isoform, and P85s6k, which is the nuclear isoform [26]. The results of the Western blot analysis indicated that the phosphorylation of the nuclear isoform P85s6k (Fig. 5A) and the ratio of p-P85s6k/P85s6k (Fig. 5C) were significantly downregulated in the LPS group, while the total P85s6k expression (Fig. 5B) showed a decreasing trend in the LPS group. However, no significant alterations were detected in p-P70s6k (Fig. 5D), P70s6k (cytoplasmic isoform; Fig. 5E), or the ratio of p-P70s6k/P70s6k (Fig. 5F). 3MA effectively prevented the reduction in P85s6k at both the expression and phosphorylation levels. These results further suggest that mTOR/P85s6k inactivation might lead to LPS-suppressed adult neurogenesis in the hippocampus.

3MA prevented the LPS-enhanced SOX2 in the hippocampus

SOX2 is a critical transcription factor in stem cells and plays an important role in the self-renewal and proliferation of NSCs [18] in the subgranular zone (SGZ) of the adult dentate gyrus. Immunofluorescence and Western blot analyses were conducted to detect the distribution and expression of SOX2, respectively. The immunofluorescence results (Fig. 6A) indicated that SOX2 (green) was detectable in the vehicle control group (Sal) and that the SOX2 signal was not restricted to the SGZ. In the LPS group, signal density and distribution of SOX2 were largely increased, particularly in the SGZ. To determine whether autophagy contributes to LPS-induced SOX2 upregulation, 3MA administration was synchronized with LPS infusion. Consistent with the immunofluorescence evidence, the protein expression of SOX2 was significantly upregulated in the hippocampus by LPS, which was prevented by 3MA treatment (Fig. 6B). These results indicate that 3MA effectively

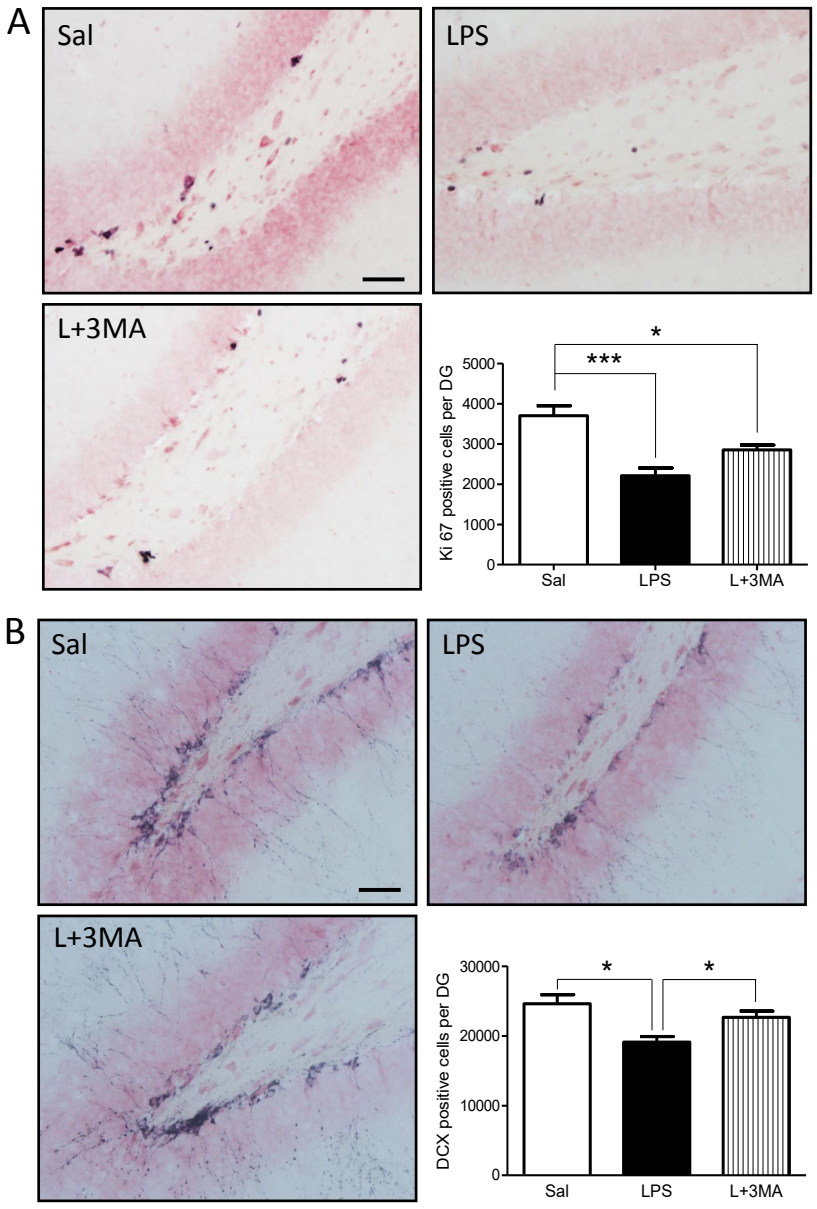

Fig. 3. A decrease in the number of Ki67-positive cells and DCX-positive cells in the dentate gyrus of LPSIP animals was prevented by icv infusion of 3MA. (A) Representative images and total number counts of Ki67-positive cells and (B) newborn neurons generated from progenitor cells (DCX-positive cells) in the subgranular zone of the dentate gyrus. Values are the mean±SEM (n=8 to 12 animals per experimental group). *p<0.05, ***p<0.001 in the *post hoc* Tukey's multiple range test. Sal: saline infusion, LPS: LPS (IP) with saline (icv), L+3MA: LPS (IP) with 3MA (icv). Scale bar: 50 μm. DCX: doublecortin.

prevented LPS-induced SOX2 expression in the hippocampus.

The LPS-altered SOX2$^+$-Beclin 1$^+$ cells in the dentate gyrus were prevented by 3MA administration

Based on the above results, we further investigated whether autophagy-associated SOX2 upregulation is an intracellular or intercellular effect by using double and triple immunofluorescence. The results from NeuN (a marker of mature neurons)-Beclin 1 immunofluorescence indicate that in the Sal group, some punctate signals of Beclin 1 (green) were located in the cytosol of neurons (red) in the granular layer of the dentate gyrus (Fig. 7A). The punctate signals of Beclin 1 in the granular layer were largely increased by LPS. The immunofluorescence of SOX2 (red)-Beclin 1 (green)-DAPI (blue) further indicated that rare SOX2$^+$-Beclin 1$^+$ cells were detected in the SGZ of the dentate gyrus in the Sal group (Fig. 7B). Notably, the number of SOX2$^+$-Beclin 1$^+$ cells (in-

https://doi.org/10.5607/en22005

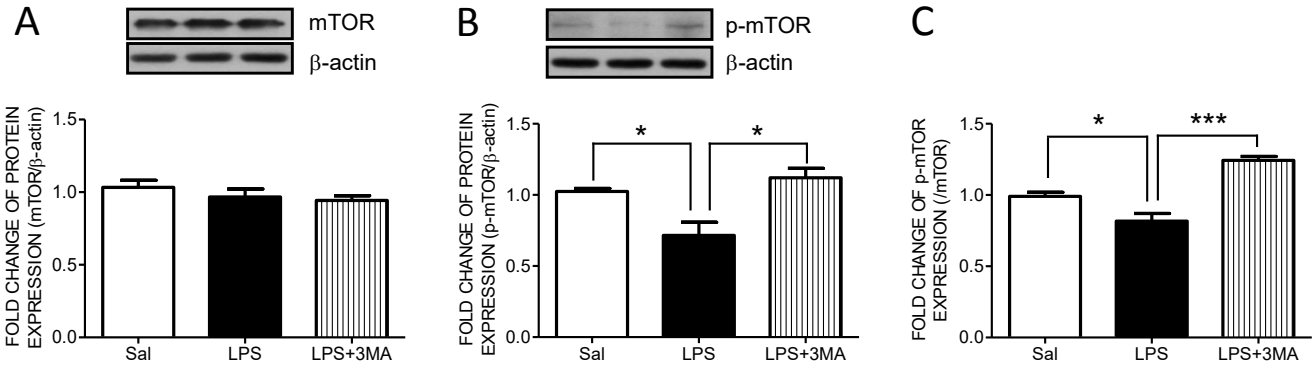

Fig. 4. The decreased protein expression of mTOR signaling in the hippocampus of animals treated with LPS was prevented by icv infusion of 3MA. Representative gels (inset) and densitometric analysis of the Western blot results showing changes in the expression of (A) mTOR, (B) phospho(p)-mTOR and the (C) p-mTOR/mTOR ratio. Values are the mean±SEM, n=10 to 12 animals per experimental group. *p<0.05, *** p< 0.001 in the *post hoc* Tukey's multiple range tests. Sal: saline infusion, LPS: LPS IP infusion with saline (icv), LPS+3MA: LPS (IP) with 3MA (icv).

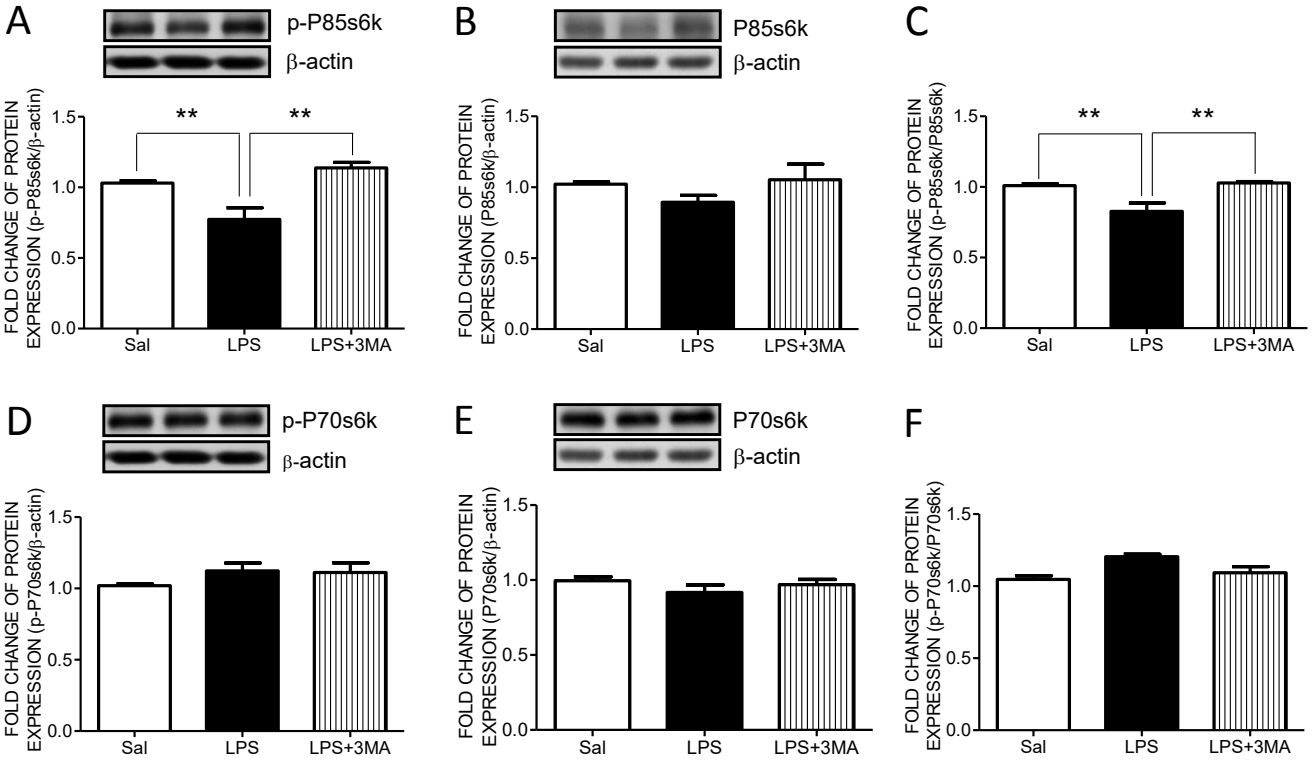

Fig. 5. Suppression of s6k in the hippocampus of animals treated with LPS peritoneal infusion was prevented by icv infusion of 3MA. The expression of (A) p-P85s6k (85 kDa; phosphorylated nuclear isoform), (B) p85s6k (nuclear isoform), (C) the p-p85s6k/p85s6k ratio, (D) p-P70s6k (70 kDa; phosphorylated cytoplasmic isoform), (E) p70s6k (cytoplasmic isoform), and (F) the p-p75s6k/p75s6k ratio in the hippocampus. Values are the mean SEM, n=10 to 12 animals per experimental group. **p<0.01 in the *post hoc* Tukey's multiple range tests. Sal: saline infusion, LPS: LPS (IP) with saline (icv) infusion, LPS+3MA: LPS (IP) with 3MA (icv).

dicated by the yellow arrowhead in the SOX2$^+$-Beclin 1$^+$ merged micrograph) was increased in the LPS group (Fig. 7B). In the LPS+3MA group, the Beclin 1 (Fig. 7A) or SOX2$^+$-Beclin 1$^+$ (Fig. 7B) signals were rarely detectable as in the Sal group. Furthermore, the observations were demonstrated by the quantification of fluorescent intensity (Table 1).

The LPS-altered SOX2$^+$-p-mTOR$^+$ cells in the dentate gyrus were prevented by 3MA administration

Furthermore, NeuN (red)-p-mTOR (green) double labeling was

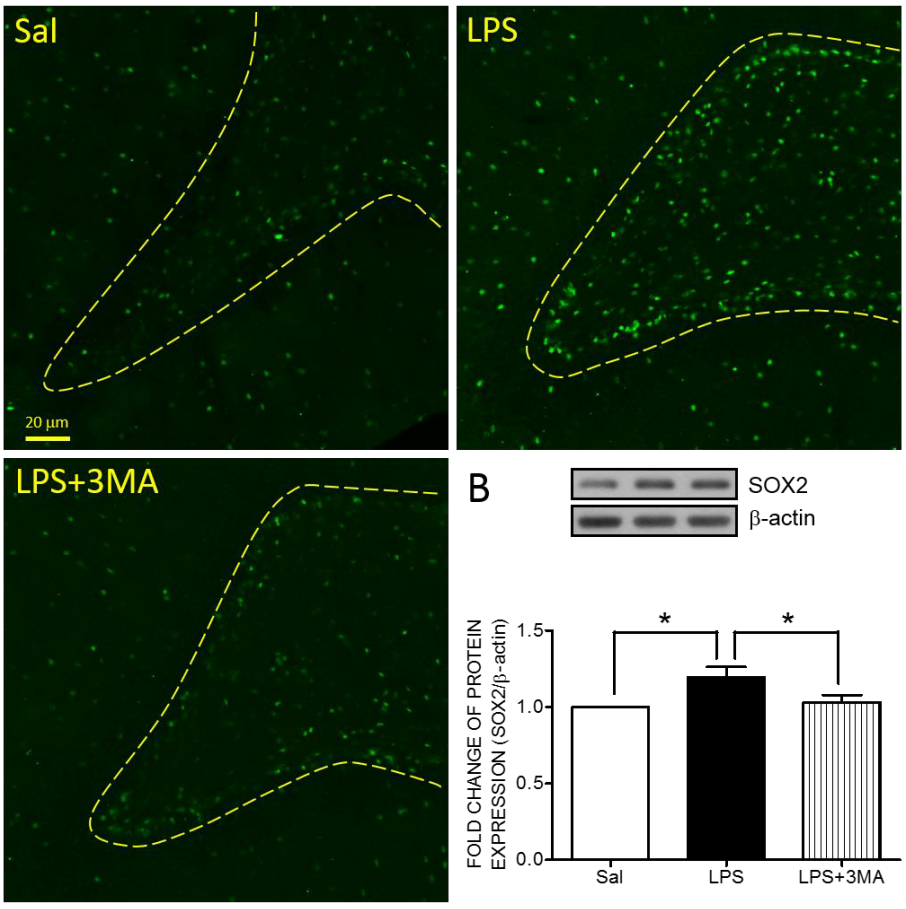

Fig. 6. The LPS-induced increase in SOX2 expression in the hippocampus was reversed by icv infusion of 3MA. (A) Representative immunofluorescence images showing the signals of SOX2 (green) in the hippocampus in the Sal, LPS, and LPS+3MA groups. (B) Representative gels (inset) and densitometric analysis of the Western blot results showing changes in the expression of SOX2. Values are the mean±SEM, n=10-12 animals per experimental group. *p<0.05 in the *post hoc* Tukey's multiple range tests. SOX2: SRY-Box Transcription Factor 2. Sal: saline infusion, LPS: LPS peritoneal infusion (IP) with saline icv infusion, LPS+3MA: LPS (IP) with 3MA (icv). icv: intracerebroventricular infusion. 3MA: 3-Methyladenine. Scale bar: 20 μm.

conducted. The results indicated that p-mTOR signals (green) were located in the cytosol of neurons (red) in the granular layer of the dentate gyrus in the Sal group (Fig. 8A). The punctate signals of p-mTOR in the granular layer were largely decreased by LPS. The images from SOX2 (red)-p-mTOR (green)-DAPI (blue) triple staining further indicated that $SOX2^+$-$p\text{-}mTOR^+$ cells (indicated by the yellow arrowhead in the $SOX2^+$-$p\text{-}mTOR^+$ merged micrograph) were primarily detected in the SGZ of the dentate gyrus in the Sal group (Fig. 8B). The number of $SOX2^+$-$p\text{-}mTOR^+$ cells was decreased in the LPS group (Fig. 8B). In the LPS+3MA group, the p-mTOR (Fig. 8A) and $SOX2^+$-$p\text{-}mTOR^+$ (Fig. 8B) signals were maintained at the same levels as those in the Sal group. The quantification data of fluorescent signals further demonstrated these image observations (Table 2).

The LPS-altered $SOX2^+$-$p\text{-}s6k^+$ cells in the dentate gyrus were prevented by 3MA administration

In addition, NeuN (red)-p-s6k (green) double labeling was conducted. Similarly, the results indicate that p-s6k signals (green) were located in the cytosol of neurons (red) in the granular layer of the dentate gyrus in the Sal group (Fig. 9A). The punctate signals of p-s6k in the granular layer were largely decreased by LPS. The images from SOX2 (red)-p-s6k (green)-DAPI (blue) triple staining further indicated that $SOX2^+$-$p\text{-}s6k^+$ cells (indicated by the yellow arrowhead in the $SOX2^+$-$p\text{-}s6k^+$ merged micrograph) were primarily detected in the SGZ of the dentate gyrus in the Sal group (Fig. 9B). The number of $SOX2^+$-$p\text{-}s6k^+$ cells was decreased in the LPS group (Fig. 9B). In the LPS+3MA group, the p-s6k (Fig. 9A) and $SOX2^+$-$p\text{-}s6k^+$ (Fig. 9B) signals were maintained at the same levels as those in the Sal group. These observations were further demonstrated by the quantification data of fluorescent signals

 https://doi.org/10.5607/en22005

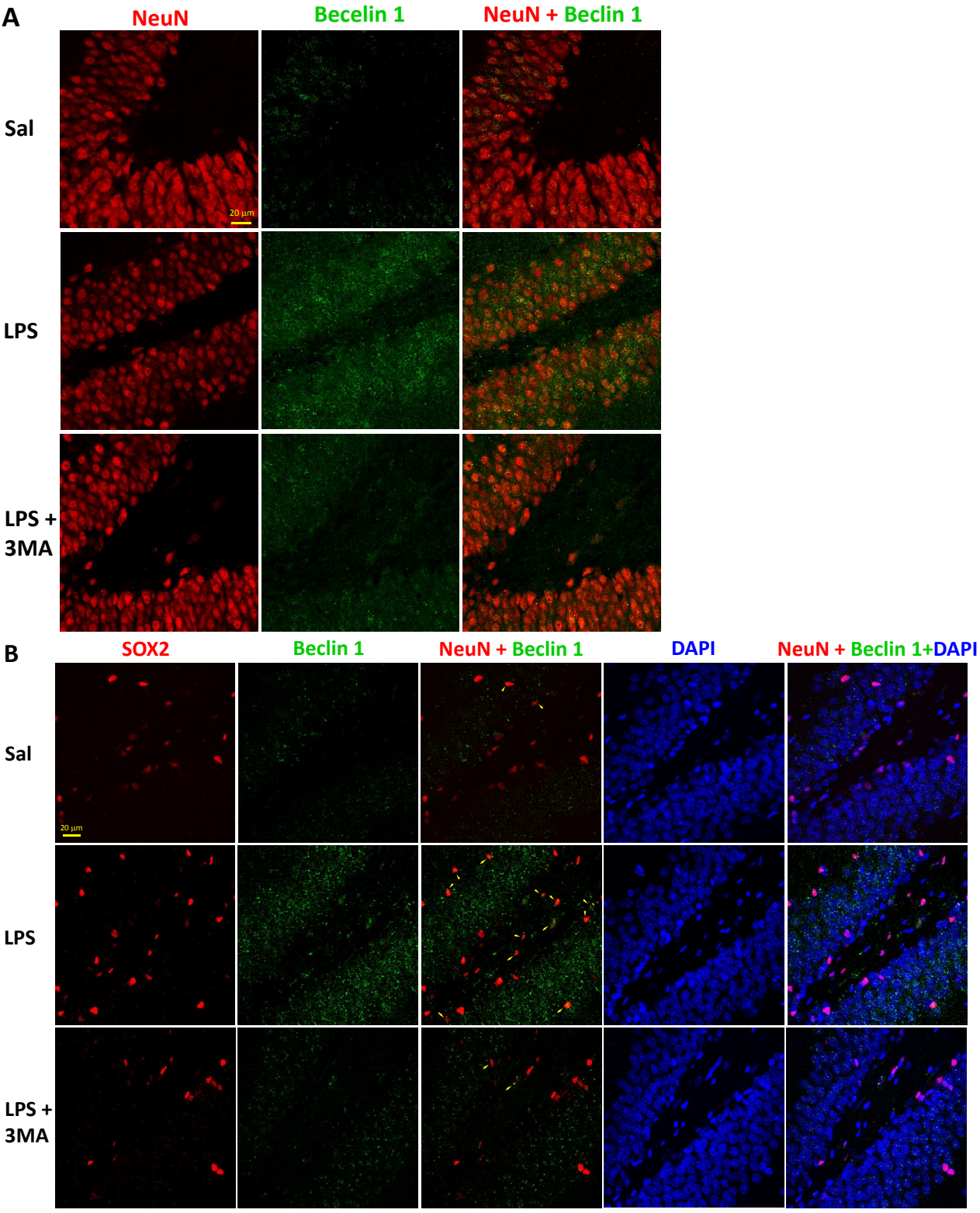

Fig. 7. The Beclin 1 signal was primarily in hippocampal neurons, and some SOX2$^+$ cells with Beclin 1$^+$ signals were in the dentate gyrus. Representative immunofluorescence images showing (A) NeuN$^+$ (red)-Beclin 1$^+$ (green), and (B) SOX2$^+$ (red)-Beclin 1$^+$ (green)-DAPI (blue) in the hippocampus in the Sal, LPS, or LPS+3MA groups. DAPI was used to identify the nuclei. Sal: saline infusion, LPS: LPS peritoneal infusion (IP) with saline icv infusion, LPS+3MA: LPS (IP) with 3MA (icv). icv: intracerebroventricular infusion. 3MA: 3-Methyladenine. SOX2: SRY-box Transcription Factor 2. Scale bar: 20 μm. Yellow arrowhead: double-labeled cells.

Table 1. Fluorescence intensity of SOX2, Beclin 1, and colocalized SOX2-Beclin 1 in the Sal, LPS and LPS+3MA groups

Fluorescence		Sal	LPS	LPS+3MA
SOX2	Area	4,889±201.0	7,474±536.2*	4,778±470.6#
	Raw intensity (RawIntDen)	786,510±40,797	1.147×10^6±75,934*	876,754±40,754#
Beclin 1	Area	2,387±460.1	12,450±2,385*	2,936±1,012#
	Raw intensity (RawIntDen)	491,331±91,594	2.567×10^6±490,572*	608,749±219,862#
SOX2+Beclin 1	Area	705±60.68	2,371±419.9**	229±79.95##
	Raw intensity (RawIntDen)	142,614±8554	426,168±63,119**	45,812±18,126##

Values are the mean±SEM, n=3 animals per experimental group. *p<0.05, **p<0.01 vs. Sal group and #p<0.05, ##p<0.01 vs. LPS group in the *post hoc* Tukey's multiple range tests. SOX2: SRY-Box Transcription Factor 2. Sal: saline infusion, LPS: LPS peritoneal infusion (IP) with saline icv infusion, LPS+3MA: LPS (IP) with 3MA (icv). icv: intracerebroventricular infusion. 3MA: 3-Methyladenine.

(Table 3). This evidence suggests that LPS-altered autophagy and mTOR signaling primarily occurred in the granular layer of the dentate gyrus and that autophagy-associated SOX2 upregulation was mostly an intercellular effect with some intercellular effect.

3MA prevented LPS-enhanced astrocytic SOX2 expression in the hippocampus

SOX2-positive NSCs are capable of differentiating into neurons or astrocytes [37, 38]. A decrease in neuronal differentiation might be a result of increased astrocytic differentiation. S100β is a marker of astrocytes at the mature stage [39]. To investigate whether LPS-induced SOX2-positive cells are prone to astrocytic differentiation under LPS, SOX2 (green) and S100β (red) double labeling was conducted. In the control group, SOX2-S100β was rarely detected (Fig. 10). Concurrent with the increased SOX2-positive cells in the dentate gyrus, the S100β signal was enhanced in the LPS group. Most importantly, the SOX2 signal was largely colocalized with the S100β signal (indicated by the yellow arrow). In the LPS+3MA group, less SOX2-S100β colocalized signal was detected in the hippocampus.

DISCUSSION

In this study, we demonstrated that the induced neuronal upregulation of Beclin 1, Atg12, SQSTM1, and LC3B-II concurrent with the downregulation of mTOR/s6k signaling contributed to an increase in SOX2-positive cells with a reduction in cell proliferation and neuronal differentiation in the adult hippocampus by sustained, low-grade peripheral LPS infusion. Intriguingly, Beclin 1^+-$SOX2^+$ cells were increased, while p-$mTOR^+$-$SOX2^+$ and $s6k^+$-$SOX2^+$ cells were reduced by LPS administration. Notably, a higher proportion of SOX2 signal was colocalized with $S100\beta^+$ astrocytes in the LPS group than in the Sal group. 3MA effectively prevented the aforementioned changes. These results suggest that neuronal autophagy might trigger SOX2 upregulation to increase NSC self-renewal and differentiation to support the existing neural circuits. Unfortunately, the autophagy-associated microenvironment might lead $SOX2^+$ cells to undergo astrogliogenesis instead of neurogenesis.

Autophagy plays dual roles in regulating NSC fates under physiological and pathological conditions [28, 40]. For instance, autophagy is involved in cell proliferation, differentiation, and maturation during neuron development. Similarly, our data further indicate that autophagy was detectable in the adult hippocampus in the control group (Sal) in this study. In contrast, the sustained activation of autophagy leads to cell death [41]. It has been reported that LPS suppresses adult neurogenesis [20] by inhibiting NSC proliferation, neural differentiation, and newborn neuron survival [30, 32-38], which have been strongly linked to the status of neuroinflammation. Our previous study demonstrated that sustained, low-grade peripheral LPS stimulation triggers neuroinflammation [26], mimicking a mild level of systemic infection. In support of previous studies [42], we demonstrated that sustained, low-grade peripheral LPS stimulation suppressed cell proliferation and neuronal differentiation in the SGZ of the dentate gyrus. 3MA prevented LPS-reduced neural differentiation and had limited capacity to prevent the suppressed cell proliferation. This evidence implies that LPS-induced autophagy might predispose to a reduction in neural differentiation in the adult hippocampus.

Beclin 1 is a critical element of the class III PI3K complex of vesicle nucleation in the autophagy pathway [20]. Atg12 is an ubiquitin-like protein involved in autophagy vesicle formation [20, 34]. SQSTM1 directly binds LC3 to facilitate autophagosome formation and sequel degradation [34]. Beclin 1, Atg12, SQSTM1 and LC3B were upregulated in the hippocampus in 7 days in this model [26]. These data imply that mild, sustained endotoxin stimulation (such as microbiota dysbiosis) could enhance the autophagy level in the hippocampus within one week. The reduction in these autophagy factors by 3MA treatment (icv) further suggests that the onsite inhibition of the initiation of PI3K complex III nucleation, vesicle elongation and autophagosome formation may be able to prevent the subsequent progression of autophagy

https://doi.org/10.5607/en22005

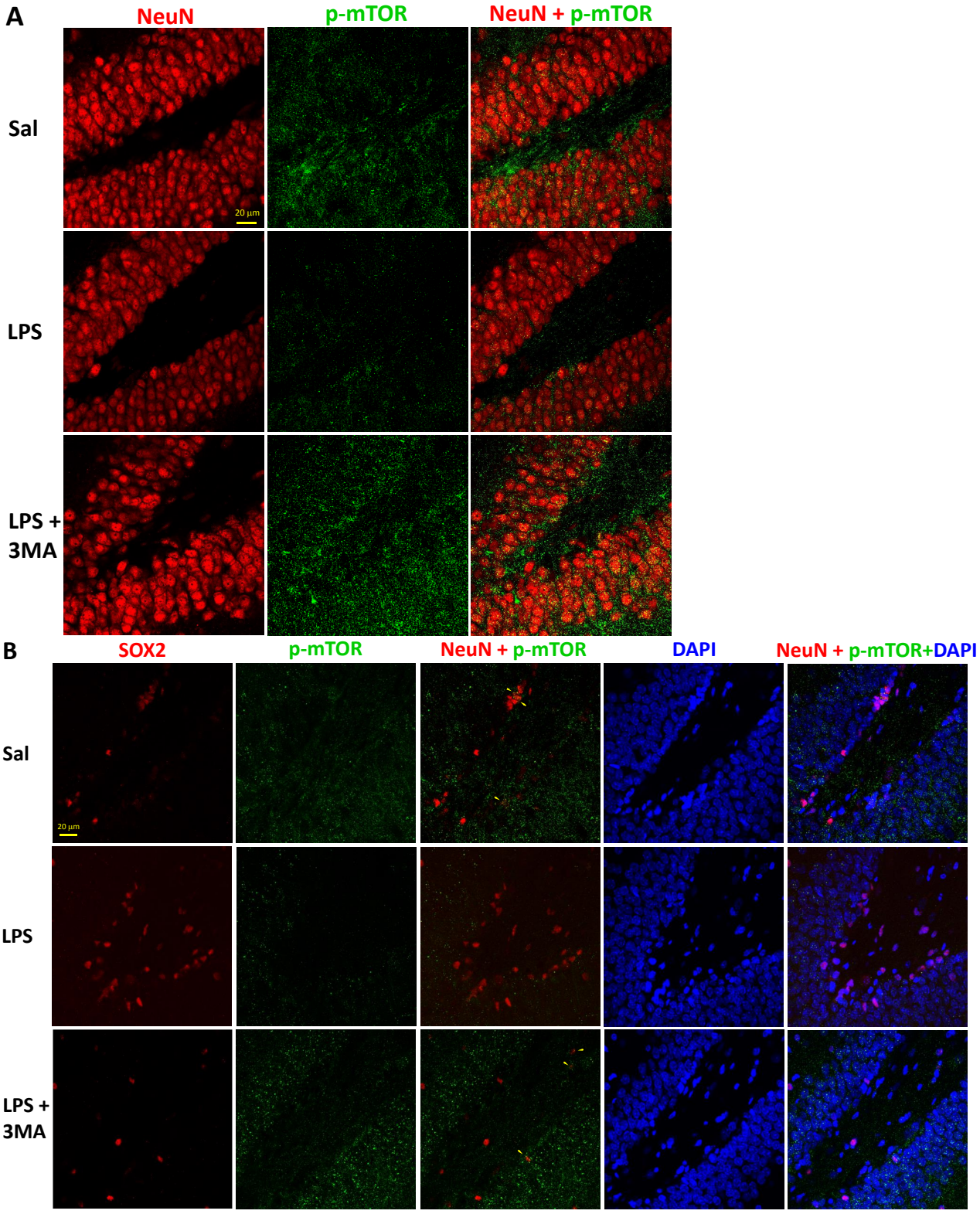

Fig. 8. The phospho(p)-mTOR signal was primarily in hippocampal neurons, and some SOX2$^+$ cells with p-mTOR$^+$ signals were in the dentate gyrus. Representative immunofluorescence images showing (A) NeuN$^+$ (red)-p-mTOR$^+$ (green), and (B) SOX2$^+$ (red)-p-mTOR$^+$ (green)-DAPI (blue) in the hippocampus in the Sal, LPS, or LPS+3MA groups. DAPI was used to identify the nuclei. Sal: saline infusion, LPS: LPS peritoneal infusion (IP) with saline icv infusion, LPS+3MA: LPS (IP) with 3MA (icv). icv: intracerebroventricular infusion. 3MA: 3-Methyladenine. p-mTOR: phospho-mTOR. SOX2: SRY-box Transcription Factor 2. Scale bar: 20 μm. Yellow arrowhead: double-labeled cells.

Table 2. Fluorescence intensity of SOX2, p-mTOR, and colocalized SOX2-p-mTOR in the Sal, LPS, and LPS+3MA groups

Fluorescence		Sal	LPS	LPS+3MA
SOX2	Area	4,700±423.3	7,077±337.5*	3,874±678.7##
	Raw intensity (RawIntDen)	904,601±69,004	1.42×10^6±86,026*	791,341±136,149##
p-mTOR	Area	9,095±639.1	2,893±510.8*	13,125±1,981###
	Raw intensity (RawIntDen)	1.961×10^6±182,704	636,602±120,655*	2.69×10^6±422,897###
SOX2+p-mTOR	Area	2,839±55.19	556±18.61***	1,724±279.1##
	Raw intensity (RawIntDen)	266,093±8,018	54,912±645.2***	153,426±21,742##

Values are the mean±SEM, n=3 animals per experimental group. *p<0.05, ***p<0.001 vs. Sal group and ##p<0.01, ###p<0.001 vs. LPS group in the *post hoc* Tukey's multiple range tests. p-mTOR: phospho-mTOR. SOX2: SRY-Box Transcription Factor 2. Sal: saline infusion, LPS: LPS peritoneal infusion (IP) with saline icv infusion, LPS+3MA: LPS (IP) with 3MA (icv). icv: intracerebroventricular infusion. 3MA: 3-Methyladenine.

and prevent impairment in neural differentiation. However, the inhibition of autophagy had no significant effect on maintaining the numbers of Ki67-positive cells in the SGZ. Our previous studies demonstrated that neuroinflammation is induced by systemic inflammation in this animal model [25, 26, 32]. Neuroinflammation sharply decreases adult hippocampal neurogenesis via activation of microglia [2]. It is well accepted that cytokines trigger Ki67-positive cell loss [43]. Therefore, it is possible that the irreversible cell proliferation in this study may be due to the sustained inflammatory microenvironment.

Notably, the wax and wane of autophagy and mTOR are crucial for the maintenance of neurogenesis. mTOR in the neural stem cell niche positively regulates downstream phospho(p)-s6k-induced protein synthesis to facilitate neuronal differentiation by the phosphorylation cascade [44]. It is conceivable that the inhibition of mTOR signaling facilitates the execution of autophagy to negatively control neurogenesis [45]. Consistent with previous studies [44, 45], our immunofluorescence data indicate that both the p-mTOR, p-s6k, and Beclin 1 signals were primarily located in the granular layer of the dentate gyrus instead of the SGZ. Combined with the semiquantification data by Western blot analysis and the distribution evidence by immunofluorescent staining, we found that the p-mTOR/p-s6k signal was higher with a low Beclin 1 signal in the Sal and LPS+3MA groups, while the intensity of the Beclin 1 signal was enhanced with a decreased p-mTOR signal in the LPS group. These results suggest an intracellular interaction between autophagy and mTOR signaling in the granular layer of the dentate gyrus. In combination with the neurogenesis evidence, these data suggest that LPS played a role in the wax and wane of autophagy and mTOR in adult hippocampal neurogenesis.

Furthermore, these data link Beclin 1 upregulation to the suppression of nuclear s6k activation and a decrease in neuronal differentiation. The nuclear isoform (85 kDa) of s6k is crucial for the regulation of gene expression [46]. It is conceivable that mild, low-grade systemic endotoxin stimulation (such as LPS leakage under microbiota dysbiosis [47]) might trigger the initiation and progression of autophagy to gradually dampen mTOR/s6k activity, leading to the suppression of neural differentiation. The mTOR/s6k signaling pathway integrates a group of molecules to regulate protein synthesis for cell growth and division, while tuberous sclerosis complex 1 (TSC1) and TSC2 antagonize mTOR signaling [22, 23, 48]. Whether the activation of TSC1 and TSC2 mediates the LPS-associated inhibition of mTOR activity in the hippocampus requires further study.

SOX2 promotes the self-renewal and proliferation of NSCs [27]. Similarly, our data further indicate that the SOX2 signal primarily accumulates in the SGZ, although it was not restricted to this area in the control group (Sal). Furthermore, we found that in the SGZ, some p-mTOR puncta (cytosol) were close to the SOX2 (nucleus) signal, while rare $SOX2^+$-Beclin 1^+ cells were detected. In contrast, SOX2 has been linked to autophagy under stress, which suppresses neurogenesis in Atg7 knockout mice [28]. Similar to a previous study [28], SOX2 signaling was significantly enhanced by LPS administration in this study. Notably, in the SGZ, the $SOX2^+$-Beclin 1^+ cells were increased when the $SOX2^+$-p-$mTOR^+$ cells were reduced by LPS administration, which is consistent with the reduced numbers of Ki67- and DCX-positive cells. These lines of evidence prominently reflect the conflicting role of SOX2 in adult neurogenesis. Notably, the Beclin 1, p-mTOR and p-s6k signals accumulate primarily in the granular layer (both the granule neurons and nonneuronal cells) of the dentate gyrus instead of the SGZ. It is possible that the upregulation of SOX2 occurs in response to the autophagy-accumulated cells in the granular layer triggering the NSC niche in the SGZ for newborn neurons to support the impaired, existing neural circuits. However, the autophagy-rich microenvironment might limit the neural differentiation ability.

Type 2 NSC cells (SOX2-positive) are precursor cells to neurons or astrocytes [37, 38]. In this study, the immunofluorescence images further suggested that the LPS-increased SOX2-positive cells were not restricted to the SGZ. A previous *in vitro* study indicated that autophagy could mediate astrogliogenesis in adult hippocampal neural stem cells [21]. Our study using double im-

https://doi.org/10.5607/en22005

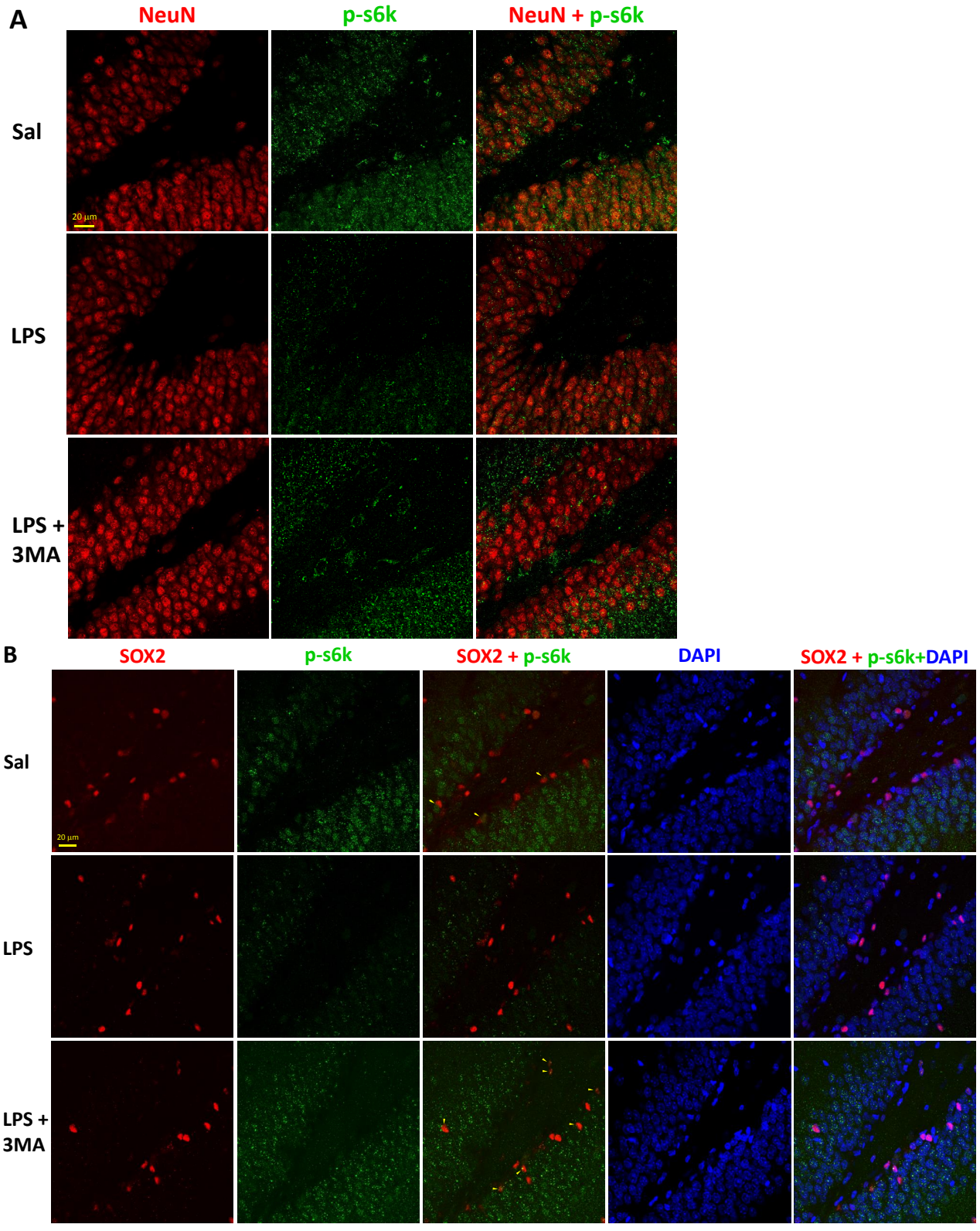

Fig. 9. The p-s6k signal was primarily in hippocampal neurons, and some $SOX2^+$-$p\text{-}s6k^+$ cells were in the dentate gyrus. Representative immunofluorescence images showing (A) $SOX2^+$ (red)-$p\text{-}s6k^+$ (green) and (B) $SOX2^+$-$p\text{-}s6k^+$ (green) in the hippocampus in the Sal, LPS, or LPS+3MA groups. DAPI (blue) was used to identify the nuclei. Sal: saline infusion, LPS: LPS peritoneal infusion (IP) with saline icv infusion, LPS+3MA: LPS (IP) with 3MA (icv). icv: intracerebroventricular infusion. 3MA: 3-Methyladenine. SOX2: SRY-box Transcription Factor 2. Scale bar: 20 μm. Yellow arrowhead: double-labeled cells.

Table 3. Fluorescence intensity of SOX2, p-S6k, and colocalized SOX2-p-S6k in the Sal, LPS and LPS+3MA groups

Fluorescence		Sal	LPS	LPS+3MA
SOX2	Area	5,228±140.2	6,877±497.9*	4,141±307.3##
	Raw intensity (RawIntDen)	1.051×10^6±22368	1.516×10^6±160,491*	837,862±19,242##
p-S6k	Area	15,923±872.4	3,222±574.2***	9,445±837.7###
	Raw intensity (RawIntDen)	3.153×106±134761	692,404±136992***	2.183×10^6±302,913##
SOX2+p-S6k	Area	2,887±211.0	465±277.8*	3,614±561.3##
	Raw intensity (RawIntDen)	635,061±26,374	99,761±61,819*	585,605±162,954#

Values are the mean±SEM, n=3 animals per experimental group. *p<0.05, ***p<0.001 vs. Sal group and #p<0.05, ##p<0.01, ###p<0.001 vs. LPS group in the *post hoc* Tukey's multiple range tests. SOX2: SRY-Box Transcription Factor 2. Sal: saline infusion, LPS: LPS peritoneal infusion (IP) with saline icv infusion, LPS+3MA: LPS (IP) with 3MA (icv). icv: intracerebroventricular infusion. 3MA: 3-Methyladenine.

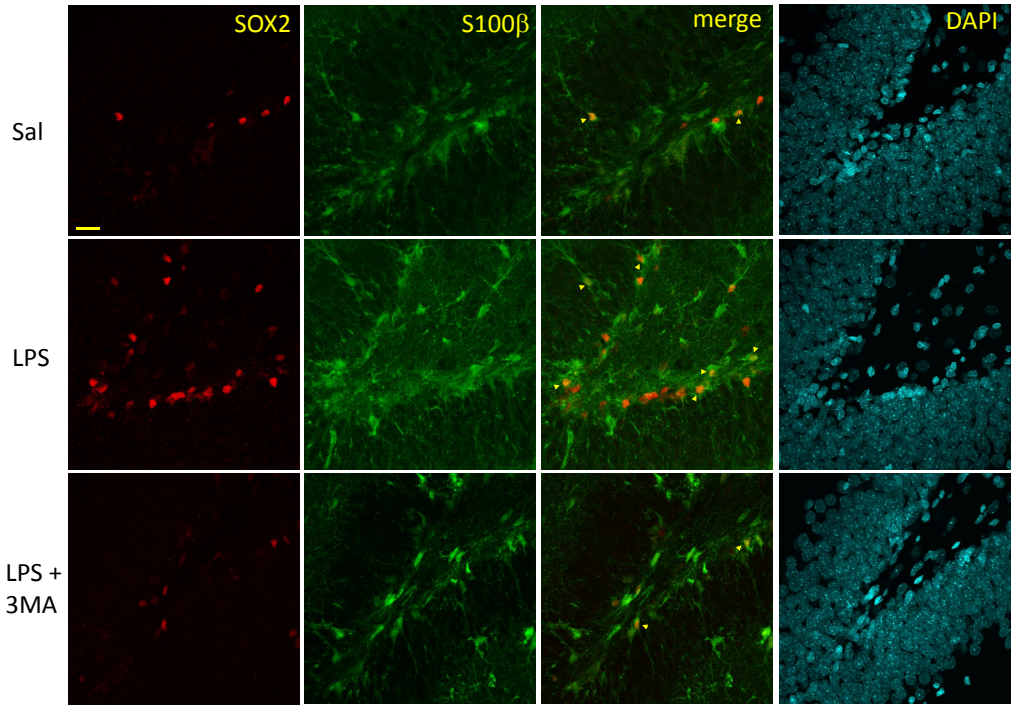

Fig. 10. The LPS-increased SOX2 signal colocalized with astrocytes in the hippocampus and was prevented by icv infusion of 3MA. Representative immunofluorescence images showing the SOX2 signal (green) colocalized with S100β in the hippocampus in the Sal, LPS, or LPS+3MA groups. DAPI (blue) was used to identify the nuclei. Sal: saline infusion, LPS: LPS peritoneal infusion (IP) with saline icv infusion, LPS+3MA: LPS (IP) with 3MA (icv). icv: intracerebroventricular infusion. 3MA: 3-Methyladenine. SOX2: SRY-Box Transcription Factor 2. Scale bar: 20 μm. Yellow arrowhead: SOX2-S100β double-labeled cells.

munofluorescence further indicates that the LPS-enhanced SOX2 signal located in astrocytes in the SGZ was increased. These lines of evidence imply that the decreased neural differentiation might be a result of increased astrocyte differentiation from SOX2-positive cells. LPS-enhanced autophagy might contribute to a switch in differentiation. Microenvironment changes, for example, LPS-reduced BDNF [49], might play roles in the waning of mTOR signaling [50] and neural differentiation [51]. Nonetheless, the interaction between neurons in the granular layer and $SOX2^+$ cells in the neural stem cell niche under LPS-induced autophagy requires further investigation.

Altogether, the data from this study indicate that LPS-impaired adult neurogenesis was mediated by the upregulation of autophagy and the suppression of mTOR/P85s6k signaling. The increased number of SOX2-positive cells contributes to the increase in astrocytic differentiation. 3MA treatment prevented LPS-associated autophagy and the inactivation of mTOR to maintain neuronal differentiation in the adult hippocampus.

ACKNOWLEDGEMENTS

This work was supported by the Kaohsiung Veterans General

Hospital, Taiwan [grant number VGHKS108-098] to WCL and the Chang Gung Memorial Hospital [grant number CMRPG8E0611] to KLHW, Taiwan, Republic of China.

ETHICS APPROVAL

All experiments were carried out in accordance with the guidelines for animal experimentation endorsed by the Institutional Animal Care and Use Committee (IACUC) of the Kaohsiung Chang Gung Memorial Hospital. IACUC number: 201506220.

CONSENT FOR PUBLICATION

Not applicable.

AVAILABILITY OF DATA AND MATERIAL

All data generated or analyzed in this study are included in this article.

AUTHORS' CONTRIBUTIONS

CWW and KLHW conceived and designed the study, analyzed, and interpreted the data, and wrote the manuscript. CWW, CYH, and ICC performed the animal experiments and tissue sampling. CWW, CYH, ICC, YCL and CYW performed the molecular analyses, data acquisition and statistical analysis. CWW, MHF, YLT, CKL, and KLHW were involved in the data interpretation. CWW and KLHW critically revised the manuscript for important intellectual content. The authors read and approved the final version of this manuscript.

DECLARATION OF INTEREST

The authors declare that they have no competing interests.

REFERENCES

1. Gage FH, Coates PW, Palmer TD, Kuhn HG, Fisher LJ, Suhonen JO, Peterson DA, Suhr ST, Ray J (1995) Survival and differentiation of adult neuronal progenitor cells transplanted to the adult brain. Proc Natl Acad Sci U S A 92:11879-11883.
2. Monje ML, Toda H, Palmer TD (2003) Inflammatory blockade restores adult hippocampal neurogenesis. Science 302:1760-1765.
3. Hanson ND, Owens MJ, Nemeroff CB (2011) Depression, antidepressants, and neurogenesis: a critical reappraisal. Neuropsychopharmacology 36:2589-2602.
4. Gould E, Beylin A, Tanapat P, Reeves A, Shors TJ (1999) Learning enhances adult neurogenesis in the hippocampal formation. Nat Neurosci 2:260-265.
5. Jaako-Movits K, Zharkovsky A (2005) Impaired fear memory and decreased hippocampal neurogenesis following olfactory bulbectomy in rats. Eur J Neurosci 22:2871-2878.
6. Jessberger S, Clark RE, Broadbent NJ, Clemenson GD Jr, Consiglio A, Lie DC, Squire LR, Gage FH (2009) Dentate gyrus-specific knockdown of adult neurogenesis impairs spatial and object recognition memory in adult rats. Learn Mem 16:147-154.
7. Kempermann G, Gage FH (2002) Genetic influence on phenotypic differentiation in adult hippocampal neurogenesis. Brain Res Dev Brain Res 134:1-12.
8. Ormerod BK, Lee TT, Galea LA (2004) Estradiol enhances neurogenesis in the dentate gyri of adult male meadow voles by increasing the survival of young granule neurons. Neuroscience 128:645-654.
9. Rola R, Raber J, Rizk A, Otsuka S, VandenBerg SR, Morhardt DR, Fike JR (2004) Radiation-induced impairment of hippocampal neurogenesis is associated with cognitive deficits in young mice. Exp Neurol 188:316-330.
10. Snyder JS, Hong NS, McDonald RJ, Wojtowicz JM (2005) A role for adult neurogenesis in spatial long-term memory. Neuroscience 130:843-852.
11. Speisman RB, Kumar A, Rani A, Foster TC, Ormerod BK (2013) Daily exercise improves memory, stimulates hippocampal neurogenesis and modulates immune and neuroimmune cytokines in aging rats. Brain Behav Immun 28:25-43.
12. Steiner B, Klempin F, Wang L, Kott M, Kettenmann H, Kempermann G (2006) Type-2 cells as link between glial and neuronal lineage in adult hippocampal neurogenesis. Glia 54:805-814.
13. Steiner B, Kronenberg G, Jessberger S, Brandt MD, Reuter K, Kempermann G (2004) Differential regulation of gliogenesis in the context of adult hippocampal neurogenesis in mice. Glia 46:41-52.
14. Woodbury ME, Freilich RW, Cheng CJ, Asai H, Ikezu S, Boucher JD, Slack F, Ikezu T (2015) miR-155 is essential for inflammation-induced hippocampal neurogenic dysfunction. J Neurosci 35:9764-9781.
15. Wu MD, Hein AM, Moravan MJ, Shaftel SS, Olschowka JA, O'Banion MK (2012) Adult murine hippocampal neurogenesis is inhibited by sustained IL-1β and not rescued by voluntary running. Brain Behav Immun 26:292-300.
16. Czapski GA, Gajkowska B, Strosznajder JB (2010) Systemic

administration of lipopolysaccharide induces molecular and morphological alterations in the hippocampus. Brain Res 1356:85-94.
17. Ekdahl CT, Claasen JH, Bonde S, Kokaia Z, Lindvall O (2003) Inflammation is detrimental for neurogenesis in adult brain. Proc Natl Acad Sci U S A 100:13632-13637.
18. Fujioka H, Akema T (2010) Lipopolysaccharide acutely inhibits proliferation of neural precursor cells in the dentate gyrus in adult rats. Brain Res 1352:35-42.
19. Wu CW, Chen YC, Yu L, Chen HI, Jen CJ, Huang AM, Tsai HJ, Chang YT, Kuo YM (2007) Treadmill exercise counteracts the suppressive effects of peripheral lipopolysaccharide on hippocampal neurogenesis and learning and memory. J Neurochem 103:2471-2481.
20. Jaeger PA, Wyss-Coray T (2009) All-you-can-eat: autophagy in neurodegeneration and neuroprotection. Mol Neurodegener 4:16.
21. Ha S, Jeong SH, Yi K, Chu JJ, Kim S, Kim EK, Yu SW (2019) Autophagy mediates astrogenesis in adult hippocampal neural stem cells. Exp Neurobiol 28:229-246.
22. Kútna V, O'Leary VB, Newman E, Hoschl C, Ovsepian SV (2021) Revisiting brain tuberous sclerosis complex in rat and human: shared molecular and cellular pathology leads to distinct neurophysiological and behavioral phenotypes. Neurotherapeutics 18:845-858.
23. Kútna V, Uttl L, Waltereit R, KrištofikováZ, Kaping D, Petrásek T, Hoschl C, Ovsepian SV (2020) Tuberous sclerosis (tsc2+/-) model Eker rats reveals extensive neuronal loss with microglial invasion and vascular remodeling related to brain neoplasia. Neurotherapeutics 17:329-339.
24. Mardhiyah I, Ardiyan YN, Aliyah SH, Sitepu EC, Herdini C, Dwianingsih EK, Asfarina F, Sumartiningsih S, Fachiroh J, Paramita DK (2021) Necrosis factor-α (TNF-α) and the presence of macrophage M2 and T regulatory cells in nasopharyngeal carcinoma. Asian Pac J Cancer Prev 22:2363-2370.
25. Fu MH, Chen IC, Lee CH, Wu CW, Lee YC, Kung YC, Hung CY, Wu KLH (2019) Anti-neuroinflammation ameliorates systemic inflammation-induced mitochondrial DNA impairment in the nucleus of the solitary tract and cardiovascular reflex dysfunction. J Neuroinflammation 16:224.
26. Wu KL, Chan SH, Chan JY (2012) Neuroinflammation and oxidative stress in rostral ventrolateral medulla contribute to neurogenic hypertension induced by systemic inflammation. J Neuroinflammation 9:212.
27. Shah K, Desilva S, Abbruscato T (2012) The role of glucose transporters in brain disease: diabetes and Alzheimer's disease. Int J Mol Sci 13:12629-12655.
28. Jung S, Choe S, Woo H, Jeong H, An HK, Moon H, Ryu HY, Yeo BK, Lee YW, Choi H, Mun JY, Sun W, Choe HK, Kim EK, Yu SW (2020) Autophagic death of neural stem cells mediates chronic stress-induced decline of adult hippocampal neurogenesis and cognitive deficits. Autophagy 16:512-530.
29. Salguero MV, Al-Obaide MAI, Singh R, Siepmann T, Vasylyeva TL (2019) Dysbiosis of Gram-negative gut microbiota and the associated serum lipopolysaccharide exacerbates inflammation in type 2 diabetic patients with chronic kidney disease. Exp Ther Med 18:3461-3469.
30. Wang J, Gu X, Yang J, Wei Y, Zhao Y (2019) Gut microbiota dysbiosis and increased plasma LPS and TMAO levels in patients with preeclampsia. Front Cell Infect Microbiol 9:409.
31. Paxinos G, Watson C (2013) The rat brain in stereotaxic coordinates. 7th ed. Academic Press, Amsterdam.
32. Wu KLH, Wu CW, Chao YM, Hung CY, Chan JYH (2016) Impaired Nrf2 regulation of mitochondrial biogenesis in rostral ventrolateral medulla on hypertension induced by systemic inflammation. Free Radic Biol Med 97:58-74.
33. Zeng X, Overmeyer JH, Maltese WA (2006) Functional specificity of the mammalian Beclin-Vps34 PI 3-kinase complex in macroautophagy versus endocytosis and lysosomal enzyme trafficking. J Cell Sci 119(Pt 2):259-270.
34. Walczak M, Martens S (2013) Dissecting the role of the Atg12-Atg5-Atg16 complex during autophagosome formation. Autophagy 9:424-425.
35. Pankiv S, Clausen TH, Lamark T, Brech A, Bruun JA, Outzen H, Øvervatn A, Bjørkøy G, Johansen T (2007) p62/SQSTM1 binds directly to Atg8/LC3 to facilitate degradation of ubiquitinated protein aggregates by autophagy. J Biol Chem 282:24131-24145.
36. Kim J, Kundu M, Viollet B, Guan KL (2011) AMPK and mTOR regulate autophagy through direct phosphorylation of Ulk1. Nat Cell Biol 13:132-141.
37. Suh H, Consiglio A, Ray J, Sawai T, D'Amour KA, Gage FH (2007) In vivo fate analysis reveals the multipotent and self-renewal capacities of Sox2+ neural stem cells in the adult hippocampus. Cell Stem Cell 1:515-528.
38. Zhao C, Deng W, Gage FH (2008) Mechanisms and functional implications of adult neurogenesis. Cell 132:645-660.
39. Raponi E, Agenes F, Delphin C, Assard N, Baudier J, Legraverend C, Deloulme JC (2007) S100B expression defines a state in which GFAP-expressing cells lose their neural stem cell potential and acquire a more mature developmental stage. Glia 55:165-177.
40. Chen X, He Y, Lu F (2018) Autophagy in stem cell biology: a perspective on stem cell self-renewal and differentiation.

Stem Cells Int 2018:9131397.
41. Nixon RA, Yang DS (2011) Autophagy failure in Alzheimer's disease--locating the primary defect. Neurobiol Dis 43:38-45.
42. Chesnokova V, Pechnick RN, Wawrowsky K (2016) Chronic peripheral inflammation, hippocampal neurogenesis, and behavior. Brain Behav Immun 58:1-8.
43. Sierra A, Encinas JM, Deudero JJ, Chancey JH, Enikolopov G, Overstreet-Wadiche LS, Tsirka SE, Maletic-Savatic M (2010) Microglia shape adult hippocampal neurogenesis through apoptosis-coupled phagocytosis. Cell Stem Cell 7:483-495.
44. Lee JE, Lim MS, Park JH, Park CH, Koh HC (2016) PTEN promotes dopaminergic neuronal differentiation through regulation of ERK-dependent inhibition of S6K signaling in human neural stem cells. Stem Cells Transl Med 5:1319-1329.
45. Casares-Crespo L, Calatayud-Baselga I, García-Corzo L, Mira H (2018) On the role of basal autophagy in adult neural stem cells and neurogenesis. Front Cell Neurosci 12:339.
46. Grove JR, Banerjee P, Balasubramanyam A, Coffer PJ, Price DJ, Avruch J, Woodgett JR (1991) Cloning and expression of two human p70 S6 kinase polypeptides differing only at their amino termini. Mol Cell Biol 11:5541-5550.
47. Mohammad S, Thiemermann C (2021) Role of metabolic endotoxemia in systemic inflammation and potential interventions. Front Immunol 11:594150.
48. Li Y, Corradetti MN, Inoki K, Guan KL (2004) TSC2: filling the GAP in the mTOR signaling pathway. Trends Biochem Sci 29:32-38.
49. Guan Z, Fang J (2006) Peripheral immune activation by lipopolysaccharide decreases neurotrophins in the cortex and hippocampus in rats. Brain Behav Immun 20:64-71.
50. Slipczuk L, Bekinschtein P, Katche C, Cammarota M, Izquierdo I, Medina JH (2009) BDNF activates mTOR to regulate GluR1 expression required for memory formation. PLoS One 4:e6007.
51. Waterhouse EG, An JJ, Orefice LL, Baydyuk M, Liao GY, Zheng K, Lu B, Xu B (2012) BDNF promotes differentiation and maturation of adult-born neurons through GABAergic transmission. J Neurosci 32:14318-14330.